

Close Examination of the Ground–State Casimir–Polder Interaction: Time–Ordered Versus Covariant Formalism and Radiative Corrections

C M Adhikari and U D Jentschura

Department of Physics, Missouri University of Science and Technology, Rolla,
Missouri 65409, USA

email: adhikaric@mst.edu, ulj@mst.edu

Abstract. The purpose of this paper is twofold. First, we compare, in detail, the derivation of the Casimir-Polder interaction using time-ordered perturbation theory, to the matching of the scattering amplitude using quantum electrodynamics. In the first case, a total of twelve time-ordered diagrams need to be considered, while in the second case, one encounters only two Feynman diagrams, namely, the ladder and crossed-ladder contributions. For ground-state interactions, we match the contribution of six of the time-ordered diagrams against the corresponding Feynman diagrams, showing the consistency of the two approaches. Second, we also examine the leading radiative correction to the long-range interaction, which is of relative order $\mathcal{O}(\alpha^3)$. In doing so, we uncover logarithmic terms, in both the interatomic distance as well as the fine-structure constant, in higher-order corrections to the Casimir–Polder interaction.

PACS numbers: 31.30.jh, 31.30.J-, 31.30.jf

Keywords: Casimir-Polder interactions, Covariant formalism, Time-ordered perturbation theory, Radiative corrections, Scattering matrix, Propagator denominator

1. Introduction

As is well known, the ground-state Casimir–Polder long-range interaction energy between atoms varies as $1/R^6$ in the short range limit, where R is interatomic distance. Due to retardation, it is of the $1/R^7$ type in the long-range regime [1]. For excited states, it has recently been shown that there are long-range tails [2] as a result of retardation.

The result for the ground state can be obtained in two completely different ways, namely, (i) using a covariant approach, with the S matrix formalism, matching the scattering amplitude against the effective Hamiltonian (ii) using so-called time-ordered perturbation theory, which actually employs time-independent field operators in the derivation and assigns a different diagram to each “time ordering” of the virtual photon emission and absorption processes. In the latter case, one encounters twelve diagrams, while in the former, only two. It would be beyond the scope of the current paper to

try to review the vast number of investigations on calculations of interatomic long-range (Casimir–Polder) potentials following the original paper [1]; let us briefly mention papers on multi-electron systems [3–5], relativistic corrections as well as other fundamental questions [6, 7], and particular aspects of excited-state interactions [8–11].

A dedicated comparison of the two approaches has been missing in the literature. One advantage of the Feynman formalism is that it clarifies, uniquely, how to encircle the poles of the atomic polarizability matrix element. Namely, the matching of the S matrix to the effective Hamiltonian leads to the Feynman prescription for encircling the poles. This realization has been instrumental in the treatment of excited reference states [2, 11], in which case some states of lower energy can become resonant, and a definite prescription is needed in order to encircle the poles correctly. However, in the time-ordered formalism, one integrates the virtual photon energies k_1 and k_2 (we set $\hbar = c = \epsilon_0 = 1$) from zero to infinity (and avoids the Feynman contour). One possibility to solve the question of how to encircle the poles, is to arrange the terms so that the characteristic factor

$$\frac{1}{k_1 + k_2} - \frac{1}{k_1 - k_2} \quad (1)$$

appears. This factor allows one to symmetrize the integrand, so that the k_2 integration then proceeds from $-\infty$ to $+\infty$. Finally, one carries out the k_2 integration by principal value. However, even after this somewhat ad hoc prescription is implemented, the result is only applicable to atoms in their ground states.

We anticipate here the result that for the ground state, the sum of six time-ordered diagrams without crossed photon lines is equal to one single “ladder” Feynman diagram. Conversely, those time-ordered diagrams that contain crossed photon lines, lead to an equal contribution as the “crossed” Feynman diagram. The universality of the end result of the derivation for the ground state means that we can take it as a safe basis for the calculation of relativistic and radiative corrections. In fact, this program has been implemented in Ref. [6]. It turns out that it is more convenient to use the length gauge for the atom-field interaction, and the so-called temporal (Weyl) gauge for the photon propagator. The Weyl gauge has the advantage over, say, the Coulomb gauge in ensuring that the 00-timelike component of the photon propagator can be ignored, while the choice of the length gauge leads to a situation where we can fortunately ignore the seagull term, proportional to \vec{A}^2 , which would otherwise have to be included in the velocity gauge.

We organize the paper as follows. In Sec. 2, we calculate the long-range interaction energy of the two-atom system using time-ordered perturbation theory. The covariant formalism, based on the matching of the scattering amplitude, is outlined in Sec. 3. In Sec. 4, we analyze the radiative corrections to the Casimir-Polder interactions. Conclusions are drawn in Sec. 5. As already stated, we use natural units with $\hbar = c = \epsilon_0 = 1$, and the electron mass is denoted by m .

2. Time-Ordered Formalism

In order to write the unperturbed Hamiltonian for a system of two neutral hydrogen atoms A and B (the generalization to multi-electron atoms is straightforward), one goes into center-of-mass coordinates and defines the relative electron coordinates (with respect to the center-of-mass) to be \vec{r}_a and \vec{r}_b , with the corresponding canonical momenta \vec{p}_a and \vec{p}_b . The unperturbed Hamiltonian is

$$\hat{H}_0 = \frac{\vec{p}_a^2}{2m_a} + V(\vec{r}_a) + \frac{\vec{p}_b^2}{2m_b} + V(\vec{r}_b) + \hat{H}_F, \quad (2)$$

Let the center-of-mass of the two atoms (roughly equal to the position vectors of the nuclei) be denoted as \vec{R}_A and \vec{R}_B . Then, if the two atoms are far enough apart such that $|\vec{r}_a|, |\vec{r}_b| \ll |\vec{R}_A - \vec{R}_B|$, the potentials $V(\vec{r}_A)$ and $V(\vec{r}_B)$ in Eq. (2) can be approximated as

$$V(\vec{r}_A) = -\frac{\alpha}{|\vec{r}_a|}, \quad V(\vec{r}_B) = -\frac{\alpha}{|\vec{r}_b|}, \quad (3)$$

where α is the fine-structure constant. Substituting $V(\vec{r}_A)$ and $V(\vec{r}_B)$ in Eq. (2), the unperturbed Hamiltonian of the system reads

$$\hat{H}_0 = \frac{\vec{p}_a^2}{2m_a} - \frac{\alpha}{|\vec{r}_a|} + \frac{\vec{p}_b^2}{2m_b} - \frac{\alpha}{|\vec{r}_b|} + \hat{H}_F. \quad (4)$$

The first two terms in Eq. (4) stand for the Schrödinger-Coulomb Hamiltonian \hat{H}_A , while the sum of the third and the fourth terms are the Schrödinger-Coulomb Hamiltonian \hat{H}_B . The electromagnetic field Hamiltonian, \hat{H}_F , is given as

$$\hat{H}_F = \sum_{\lambda=1}^2 \int d^3k \, k \, a_{\lambda}^{\dagger}(\vec{k}) a_{\lambda}(\vec{k}). \quad (5)$$

Here a_{λ}^{\dagger} and a_{λ} are the usual creation and annihilation operators, which satisfy the following commutation relation:

$$\left[a_{\lambda}(\vec{k}), a_{\lambda'}^{\dagger}(\vec{k}') \right] = \delta^{(3)}(\vec{k} - \vec{k}') \delta_{\lambda\lambda'}. \quad (6)$$

Along with the dipole approximation, the interaction Hamiltonian in the so-called length gauge of quantum electrodynamics (QED) is approximated as

$$\hat{H}_{AB} \approx -e \vec{r}_a \cdot \vec{E}(\vec{R}_A) - e \vec{r}_b \cdot \vec{E}(\vec{R}_B), \quad (7)$$

where $\vec{E}(\vec{R}_A)$ and $\vec{E}(\vec{R}_B)$ are the (Schrödinger-picture, time-independent, see Ref. [12]) electric field operators. In writing Eq. (7), we implicitly assume that the wavelength of the exchanged virtual photon is much longer than the dimension of the atom, so that the electric-field operator can be taken at the center-of-mass of the atom. Furthermore, the electromagnetic interaction of the proton is taken into account by using the relative coordinates \vec{r}_a and \vec{r}_b rather than the electron coordinates. Finally, the electromagnetic-field operators are given by

$$\vec{E}(\vec{R}_A) = \sum_{\lambda=1}^2 \int \frac{d^3k}{(2\pi)^{3/2}} \sqrt{\frac{k}{2}} \hat{\epsilon}_{\lambda}(\vec{k}) \left[i a_{\lambda}(\vec{k}) e^{i\vec{k} \cdot \vec{R}_A} - i a_{\lambda}^{\dagger}(\vec{k}) e^{-i\vec{k} \cdot \vec{R}_A} \right], \quad (8)$$

and

$$\vec{E}(\vec{R}_B) = \sum_{\lambda=1}^2 \int \frac{d^3k}{(2\pi)^{3/2}} \sqrt{\frac{k}{2}} \hat{\epsilon}_{\lambda}(\vec{k}) \left[i a_{\lambda}(\vec{k}) e^{i\vec{k} \cdot \vec{R}_B} - i a_{\lambda}^{\dagger}(\vec{k}) e^{-i\vec{k} \cdot \vec{R}_B} \right]. \quad (9)$$

In terms of the creation, annihilation operators of the field, the interaction Hamiltonian of the system becomes

$$\begin{aligned} \hat{H}_{AB} = & -e \sum_{\lambda=1}^2 \int \frac{d^3k}{(2\pi)^{3/2}} \sqrt{\frac{k}{2}} \left[\left(i a_{\lambda}(\vec{k}) \hat{\epsilon}_{\lambda}(\vec{k}) e^{i\vec{k} \cdot \vec{R}_A} - i a_{\lambda}^{\dagger}(\vec{k}) \hat{\epsilon}_{\lambda}(\vec{k}) e^{-i\vec{k} \cdot \vec{R}_A} \right) \cdot \vec{r}_a \right. \\ & \left. + \left(i a_{\lambda}(\vec{k}) \hat{\epsilon}_{\lambda}(\vec{k}) e^{i\vec{k} \cdot \vec{R}_B} - i a_{\lambda}^{\dagger}(\vec{k}) \hat{\epsilon}_{\lambda}(\vec{k}) e^{-i\vec{k} \cdot \vec{R}_B} \right) \cdot \vec{r}_b \right]. \end{aligned} \quad (10)$$

The reference state $|\phi_0\rangle = |\phi_{1S,A}, \phi_{1S,B}, 0\rangle$ has both atoms A and B in their ground states and the electromagnetic field in the vacuum state $|0\rangle$. We here calculate the perturbation effect of the interaction Hamiltonian. The orthonormality condition for the atomic parts of the combined atom+field state is

$$\langle n|m\rangle = \delta_{nm}, \quad (11)$$

where δ_{nm} is the Kronecker delta and $|n\rangle$ and $|m\rangle$ are any atomic eigenstates of the atomic part of the unperturbed Hamiltonian \hat{H}_0 , for either atom A or B . In the following, we reserve the notation $|\sigma\rangle$ for a virtual state of atom A , while a virtual state of atom B is denoted as $|\rho\rangle$. It is easy to see that all odd-order perturbations involving the Hamiltonian (7) vanish. The second-order terms are the sum of self-energy effects (when both field operators act on the same atom), as well as one-photon exchange terms which are relevant only if one has an energetically degenerate, or quasi-degenerate, state available in either atom, which can be reached via a dipole transition [10]; this is typically the case only when excited reference states are involved [8–11]. Thus, we look into the fourth order perturbation, which reads

$$\Delta E^{(4)} = \left\langle \phi_0 \left| \hat{H}_{AB} \frac{1}{(E_0 - \hat{H}_0)'} \hat{H}_{AB} \frac{1}{(E_0 - \hat{H}_0)'} \hat{H}_{AB} \frac{1}{(E_0 - \hat{H}_0)'} \hat{H}_{AB} \right| \phi_0 \right\rangle. \quad (12)$$

The prime in the operator $\frac{1}{(E_0 - \hat{H}_0)'}$ indicates that the reference state is excluded from the spectral decomposition of the operator. The virtual states which need to be used in the calculation of the fourth-order perturbation (12) carry one, and two photons in the electromagnetic field modes.

A Casimir-Polder interaction between two atoms A and B involving two virtual photons results in four different types of intermediate states, namely, (1) Both atoms are in ground states, and two virtual photons are present, (2) Only one atom is in the excited state, and only one virtual photon is exchanged, (3) Both atoms are in the excited state, but no photon is present, and (4) Both atoms are in the excited state, and two photons are present [13, 14]. Thus, the electrons and photons can couple in $4 \times 3 \times 2 \times 1 = 12$ distinct ways. Fig. 1 represents all these 12 time-ordered sequences of the interaction.

Let us first investigate the first diagram of the Fig. 1. There are four factors which give contributions to the interaction energy, namely, emission of \vec{k}_2 at R_B , emission

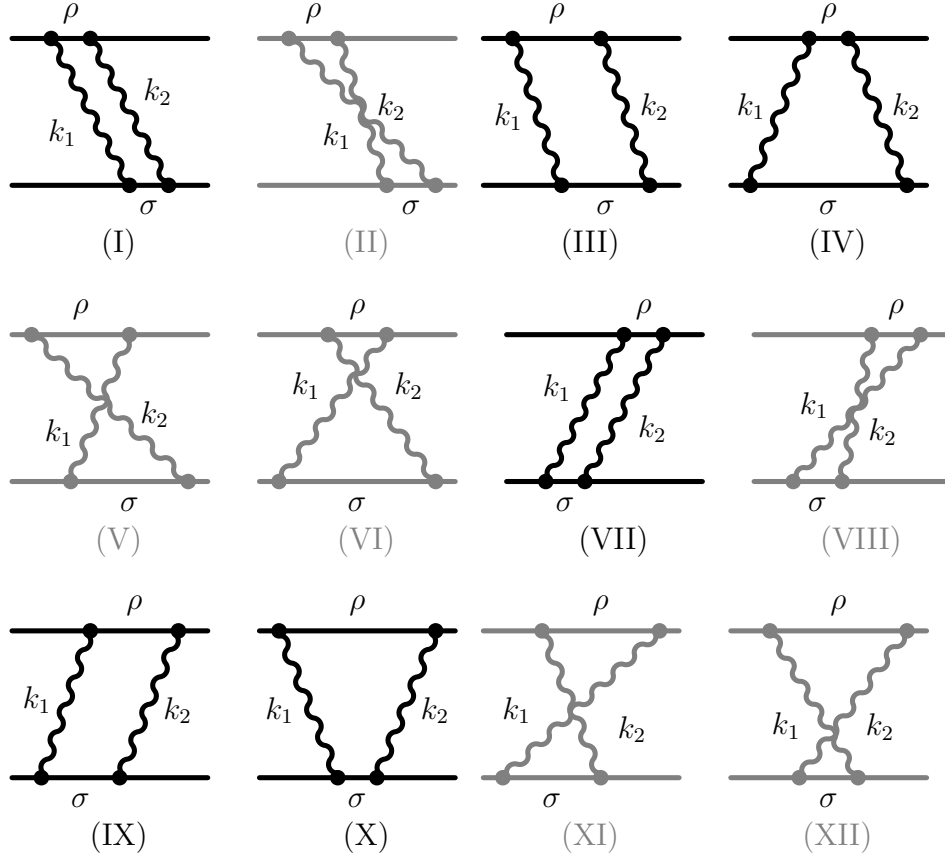


Figure 1. Time-ordered diagrams showing the Casimir-Polder interaction between two atoms A and B . The ρ and σ lines are the virtual states associated with the atom A and the atom B . The k_1 and k_2 are the magnitude of the momenta of the photons to the left and to the right of the line respectively.

of \vec{k}_1 at R_B , absorption of \vec{k}_2 at R_A , and absorption of \vec{k}_1 at R_A . The corresponding fourth-order energy shift reads

$$\begin{aligned} \Delta E_I^{(4)} = & e^4 \int \frac{d^3 k_1}{(2\pi)^3} \int \frac{d^3 k_2}{(2\pi)^3} \sum_{\lambda_1, \lambda_2} \sum_{\rho, \sigma} \frac{k_1 k_2}{4} (i) \langle \phi_{1S,A} | \hat{\epsilon}_{\lambda_1}(\vec{k}_1) \cdot \vec{r}_a | \rho \rangle e^{i\vec{k}_1 \cdot \vec{R}_A} (-i) \\ & \times \langle \phi_{1S,B} | \hat{\epsilon}_{\lambda_1}(\vec{k}_1) \cdot \vec{r}_b | \sigma \rangle e^{-i\vec{k}_1 \cdot \vec{R}_B} (i) \langle \rho | \hat{\epsilon}_{\lambda_2}(\vec{k}_2) \cdot \vec{r}_a | \phi_{1S,A} \rangle e^{i\vec{k}_2 \cdot \vec{R}_A} (-i) \\ & \times \langle \sigma | \hat{\epsilon}_{\lambda_2}(\vec{k}_2) \cdot \vec{r}_b | \phi_{1S,B} \rangle e^{-i\vec{k}_2 \cdot \vec{R}_B} \frac{1}{(E_{1S,A} - E_\rho - k_1)(-k_1 - k_2)(E_{1S,B} - E_\sigma - k_2)}, \quad (13) \end{aligned}$$

where $|\phi_{1S,i}\rangle$, $i = A, B$ is a ket associated to the ground state of the atom i . The summation over the virtual states $|\rho\rangle$ and $|\sigma\rangle$ of atoms A and B includes an integral over the continuous spectrum. Atom B undergoes the transition $|1S, B\rangle \rightarrow |\sigma\rangle \rightarrow |1S, B\rangle$, each time under the emission of photons, while atom A undergoes the transition $|1S, A\rangle \rightarrow |\rho\rangle \rightarrow |1S, A\rangle$, each time under the absorption of a photon. We have used Eqs. (7)–(10).

The polarization vectors $\hat{\epsilon}_{\lambda_i}(\vec{k}_i)$, with $i = 1, 2$, satisfy the following identities,

$$\hat{\epsilon}_{\lambda_i}(\vec{k}) \cdot \hat{\epsilon}_{\lambda_j}(\vec{k}) = \delta_{\lambda_i \lambda_j}, \quad \vec{k} \cdot \hat{\epsilon}_{\lambda_i}(\vec{k}) = 0, \quad \sum_{\lambda_i=1}^2 \hat{\epsilon}_{\lambda_i}^p(\vec{k}_r) \hat{\epsilon}_{\lambda_i}^q(\vec{k}_r) = \delta^{pq} - \frac{k_r^p k_r^q}{k_r^2}. \quad (14)$$

Thus, the contribution to the interaction energy from the first diagram reads

$$\begin{aligned} \Delta E_I^{(4)} = & e^4 \int \frac{d^3 k_1}{(2\pi)^3} \int \frac{d^3 k_2}{(2\pi)^3} \frac{k_1 k_2}{4} \left(\delta^{mr} - \frac{k_1^m k_1^r}{k_1^2} \right) \left(\delta^{ns} - \frac{k_2^n k_2^s}{k_2^2} \right) e^{i(\vec{k}_1 + \vec{k}_2) \cdot \vec{R}} \\ & \times \sum_{\rho, \sigma} \frac{\langle \phi_{1S,A} | x^m | \rho \rangle \langle \rho | x^n | \phi_{1S,A} \rangle \langle \phi_{1S,B} | x^r | \sigma \rangle \langle \sigma | x^s | \phi_{1S,B} \rangle}{(E_{1S,A} - E_\rho - k_1)(-k_1 - k_2)(E_{1S,B} - E_\sigma - k_2)}, \end{aligned} \quad (15)$$

where $\vec{R} = \vec{R}_A - \vec{R}_B$ is the internuclear separation. If we denote a propagator denominator by \mathcal{D}_K , where K is the roman numeral identifying a diagram in Fig. 1, then for diagram (I), we have,

$$\mathcal{D}_I = (E_{1S,A} - E_\rho - k_1)(-k_1 - k_2)(E_{1S,B} - E_\sigma - k_2). \quad (16)$$

Note that in the virtual state in the “middle” of diagram I, both atoms are in the ground state.

The net fourth order energy shift of the system is the sum of the contributions of all the 12 diagrams. Explicitly,

$$\begin{aligned} \Delta E^{(4)} = & e^4 \int \frac{d^3 k_1}{(2\pi)^3} \int \frac{d^3 k_2}{(2\pi)^3} \frac{k_1 k_2}{4} \left(\delta^{mr} - \frac{k_1^m k_1^r}{k_1^2} \right) \left(\delta^{ns} - \frac{k_2^n k_2^s}{k_2^2} \right) e^{i(\vec{k}_1 + \vec{k}_2) \cdot \vec{R}} \\ & \times \sum_{\rho, \sigma} \langle \phi_{1S,A} | x^m | \rho \rangle \langle \rho | x^n | \phi_{1S,A} \rangle \langle \phi_{1S,B} | x^r | \sigma \rangle \langle \sigma | x^s | \phi_{1S,B} \rangle \sum_{j=1}^{XII} \mathcal{D}_j^{-1}. \end{aligned} \quad (17)$$

The six diagrams we want to study first are I, III, IV, VII, IX, and X. The rationale behind the grouping is that the photon-lines of the six mentioned time-ordered diagrams do not cross (they are the dark-colored in Fig. 1). By contrast, photon lines cross in the rest of other six diagrams (gray diagrams of Fig. 1). Our treatment is inspired by Ref. [13] but specialized to the mentioned sets of time-ordered diagrams.

Let us look at the diagram III, which is the second time-ordered diagram without a photon-line crossing (see Fig. 1). The diagram III involves the emission of a photon with wave vector \vec{k}_2 at \vec{R}_B , the emission of \vec{k}_1 at \vec{R}_A , and the excitation of both atoms. Thus, the propagator denominator (\mathcal{D}_{III}) corresponding to the diagram (III) reads

$$\mathcal{D}_{III} = (E_{1S,A} - E_\rho - k_1)(E_{1S,A} - E_\sigma + E_{1S,B} - E_\rho)(E_{1S,B} - E_\sigma - k_2). \quad (18)$$

The corresponding energy shift is

$$\begin{aligned} \Delta E_{III}^{(4)} = & e^4 \int \frac{d^3 k_1}{(2\pi)^3} \int \frac{d^3 k_2}{(2\pi)^3} \frac{k_1 k_2}{4} \left(\delta^{mr} - \frac{k_1^m k_1^r}{k_1^2} \right) \left(\delta^{ns} - \frac{k_2^n k_2^s}{k_2^2} \right) e^{i(\vec{k}_1 + \vec{k}_2) \cdot \vec{R}} \\ & \times \sum_{\rho, \sigma} \frac{\langle \phi_{1S,A} | x^m | \rho \rangle \langle \rho | x^n | \phi_{1S,A} \rangle \langle \phi_{1S,B} | x^r | \sigma \rangle \langle \sigma | x^s | \phi_{1S,B} \rangle}{(E_{1S,A} - E_\rho - k_1)(E_{1S,A} - E_\sigma + E_{1S,B} - E_\rho)(E_{1S,B} - E_\sigma - k_2)}. \end{aligned} \quad (19)$$

The propagator denominators \mathcal{D}_{IV} , \mathcal{D}_{VII} , \mathcal{D}_{IX} , and \mathcal{D}_X , of the diagrams IV, VII, IX, and X in Fig. 1, respectively, are given by

$$\mathcal{D}_{IV} = (E_{1S,B} - E_\sigma - k_1)(E_{1S,A} - E_\rho + E_{1S,B} - E_\sigma)(E_{1S,B} - E_\sigma - k_2), \quad (20a)$$

$$\mathcal{D}_{VII} = (E_{1S,B} - E_\sigma - k_1)(-k_1 - k_2)(E_{1S,A} - E_\rho - k_2), \quad (20b)$$

$$\mathcal{D}_{IX} = (E_{1S,B} - E_\sigma - k_1)(E_{1S,A} - E_\rho + E_{1S,B} - E_\sigma)(E_{1S,A} - E_\rho - k_2), \quad (20c)$$

$$\mathcal{D}_X = (E_{1S,A} - E_\rho - k_1)(E_{1S,A} - E_\rho + E_{1S,B} - E_\sigma)(E_{1S,A} - E_\rho - k_2). \quad (20d)$$

For simplicity, we denote $E_\rho - E_{1S,A} = E_{A\rho}$ and $E_\sigma - E_{1S,B} = E_{B\sigma}$.

Let us now group, simplify, and then assemble the propagator denominators as below:

$$\frac{1}{\mathcal{D}_I} + \frac{1}{\mathcal{D}_{III}} = \frac{1}{k_1 + k_2} \left(\frac{-1}{(E_{A\rho} + E_{B\sigma})(E_{B\sigma} + k_2)} + \frac{-1}{(E_{A\rho} + E_{B\sigma})(E_{A\rho} + k_1)} \right), \quad (21a)$$

$$\mathcal{D}_{IV}^{-1} = \frac{1}{E_{A\rho} + E_{B\sigma}} \left(\frac{1}{E_{B\sigma} + k_1} - \frac{1}{E_{B\sigma} + k_2} \right) \frac{1}{k_1 - k_2}, \quad (21b)$$

$$\frac{1}{\mathcal{D}_{VII}} + \frac{1}{\mathcal{D}_{IX}} = \frac{1}{k_1 + k_2} \left(\frac{-1}{(E_{A\rho} + E_{B\sigma})(E_{B\sigma} + k_1)} + \frac{-1}{(E_{A\rho} + E_{B\sigma})(E_{A\rho} + k_2)} \right), \quad (21c)$$

$$\mathcal{D}_X^{-1} = \frac{1}{E_{A\rho} + E_{B\sigma}} \left(\frac{1}{E_{A\rho} + k_1} - \frac{1}{E_{A\rho} + k_2} \right) \frac{1}{k_1 - k_2}. \quad (21d)$$

Adding Eqs. (21a)–(21d) and simplifying, we obtain for the “ladder” (hence the subscript L) contribution,

$$\begin{aligned} D_L^{-1} &= \mathcal{D}_I^{-1} + \mathcal{D}_{III}^{-1} + \mathcal{D}_{IV}^{-1} + \mathcal{D}_{VII}^{-1} + \mathcal{D}_{IX}^{-1} + \mathcal{D}_X^{-1} \\ &= -\frac{1}{(E_{A\rho} + E_{B\sigma})} \left(\frac{1}{E_{A\rho} + k_1} + \frac{1}{E_{B\sigma} + k_1} \right) \left(\frac{1}{k_1 + k_2} - \frac{1}{k_1 - k_2} \right) \\ &\quad - \frac{1}{(E_{A\rho} + E_{B\sigma})} \left(\frac{1}{E_{A\rho} + k_2} + \frac{1}{E_{B\sigma} + k_2} \right) \left(\frac{1}{k_1 + k_2} + \frac{1}{k_1 - k_2} \right). \end{aligned} \quad (22)$$

We see the characteristic factor (1) emerge. Furthermore, we notice that the second term is equivalent to the first, which implies that the terms lead to equivalent contributions under the photon integral.

The fourth order energy shift due to the six time-ordered diagrams I, III, IV, VII, IX, and X, simplifies to

$$\begin{aligned} E_L(R) &= -e^4 \int \frac{d^3 k_1}{(2\pi)^3} \int \frac{d^3 k_2}{(2\pi)^3} \frac{k_1 k_2}{4} \left(\delta^{mr} - \frac{k_1^m k_1^r}{k_1^2} \right) \left(\delta^{ns} - \frac{k_2^n k_2^s}{k_2^2} \right) e^{i(\vec{k}_1 + \vec{k}_2) \cdot \vec{R}} \\ &\quad \times \sum_{\rho, \sigma} \langle \phi_{1S,A} | x^m | \rho \rangle \langle \rho | x^n | \phi_{1S,A} \rangle \langle \phi_{1S,B} | x^r | \sigma \rangle \langle \sigma | x^s | \phi_{1S,B} \rangle \mathcal{D}_L^{-1} \\ &= -\frac{e^4}{18} \int \frac{d^3 k_1}{(2\pi)^3} \int \frac{d^3 k_2}{(2\pi)^3} k_1 k_2 \delta^{mn} \delta^{rs} \left(\delta^{mr} - \frac{k_1^m k_1^r}{k_1^2} \right) \left(\delta^{ns} - \frac{k_2^n k_2^s}{k_2^2} \right) e^{i(\vec{k}_1 + \vec{k}_2) \cdot \vec{R}} \\ &\quad \times \sum_{\rho, \sigma} \sum_{j, \ell} \langle \phi_{1S,A} | x^j | \rho \rangle \langle \rho | x^j | \phi_{1S,A} \rangle \langle \phi_{1S,B} | x^\ell | \sigma \rangle \langle \sigma | x^\ell | \phi_{1S,B} \rangle \\ &\quad \times \frac{(E_{A\rho} + E_{B\sigma} + 2k_1)}{(E_{A\rho} + E_{B\sigma})(E_{B\sigma} + k_1)(E_{A\rho} + k_1)} \left(\frac{1}{k_1 + k_2} - \frac{1}{k_1 - k_2} \right), \end{aligned} \quad (23)$$

where we have used the following identity

$$\sum_{i,j} \langle \phi_{1S,A} | x^i | \rho \rangle \langle \rho | x^j | \phi_{1S,A} \rangle = \frac{\delta^{ij}}{3} \sum_s \langle \phi_{1S,A} | x^s | \rho \rangle \langle \rho | x^s | \phi_{1S,A} \rangle, \quad (24)$$

which is valid for any S state. Using the identity $\int d^3k = \int_0^\infty k^2 dk \int d\Omega$, where $d\Omega = \sin\theta d\theta d\phi$, the angular part of Eq. (23) can be integrated as

$$\begin{aligned} & \int_0^\pi \sin\theta d\theta \int_0^{2\pi} d\phi \left(\delta^{mr} - \frac{k_1^m k_1^r}{k_1^2} \right) e^{i\vec{k}_1 \cdot \vec{R}} \\ &= 4\pi \left[\left(\delta^{mr} - \frac{R^m R^r}{R^2} \right) \frac{\sin k_1 R}{k_1 R} + \left(\delta^{mr} - 3 \frac{R^m R^r}{R^2} \right) \left(\frac{\cos k_1 R}{(k_1 R)^2} - \frac{\sin k_1 R}{(k_1 R)^3} \right) \right]. \end{aligned} \quad (25)$$

With the help of Eq. (25), Eq. (23) can be re-expressed as

$$\begin{aligned} E_L(R) &= \frac{-e^4}{36\pi^4} \sum_{\rho,\sigma} \sum_{j,\ell} \frac{\langle \phi_{1S,A} | x^j | \rho \rangle \langle \rho | x^j | \phi_{1S,A} \rangle \langle \phi_{1S,B} | x^\ell | \sigma \rangle \langle \sigma | x^\ell | \phi_{1S,B} \rangle}{(E_{A\rho} + E_{B\sigma})} \int_0^\infty dk_1 A^{mr}(k_1 R) \\ &\times \frac{k_1^3 (E_{A\rho} + E_{B\sigma} + 2k_1)}{(E_{B\sigma} + k_1)(E_{A\rho} + k_1)} \delta^{mn} \delta^{rs} \left(\int_0^\infty dk_2 k_2^3 \frac{A^{ns}(k_2 R)}{(k_1 + k_2)} - \int_0^\infty dk_2 k_2^3 \frac{A^{ns}(k_2 R)}{(k_1 - k_2)} \right), \end{aligned} \quad (26)$$

where

$$A^{ns}(x) = \left(\delta^{ns} - \frac{R^n R^s}{R^2} \right) \frac{\sin x}{x} + \left(\delta^{ns} - 3 \frac{R^n R^s}{R^2} \right) \left(\frac{\cos x}{x^2} - \frac{\sin x}{x^3} \right) \quad (27)$$

is an even function of x , which allows us to extend the integration limit from $k_2 = -\infty$ to $k_2 = +\infty$. Consequently, we have

$$\begin{aligned} E_L(R) &= -\frac{e^4}{72\pi^4} \sum_{\rho,\sigma} \sum_{j,\ell} \frac{1}{E_{A\rho} + E_{B\sigma}} \langle \phi_{1S,A} | x^j | \rho \rangle \langle \rho | x^j | \phi_{1S,A} \rangle \langle \phi_{1S,B} | x^\ell | \sigma \rangle \langle \sigma | x^\ell | \phi_{1S,B} \rangle \\ &\times \int_0^\infty dk_1 k_1^3 \delta^{mn} \delta^{rs} A^{mr}(k_1 R) \frac{(E_{A\rho} + E_{B\sigma} + 2k_1)}{(E_{B\sigma} + k_1)(E_{A\rho} + k_1)} \int_{-\infty}^\infty dk_2 k_2^3 \frac{A^{ns}(k_2 R)}{(k_1 + k_2)}, \end{aligned} \quad (28)$$

where we have used the symmetry of the integrand in order to extend the integration limits to the interval $-\infty < k_2 < \infty$. The k_2 -integral has a pole of order one at $k_2 = -k_1$. Strictly speaking, the k_2 integral in Eq. (28) is not uniquely defined, and its value depends on the integration prescription. In the following, we shall implicitly assume that a principal-value prescription is indicated. Let $k_2 R = x$ and $k_1 R = x_1$. Then the k_2 -integral can be written as

$$\begin{aligned} & \int_{-\infty}^\infty dk_2 k_2^3 \frac{A^{ns}(k_2 R)}{(k_1 + k_2)} \\ &= \frac{1}{R^3} \left(\delta^{ns} - \frac{R^n R^s}{R^2} \right) \lim_{\eta \rightarrow 0} \left\{ \int_{-\infty}^\infty dx \frac{x^2}{x + x_1} \frac{e^{ix - \eta|x|}}{2i} - \int_{-\infty}^\infty dx \frac{x^2}{x + x_1} \frac{e^{-ix - \eta|x|}}{2i} \right\} \\ &+ \frac{1}{R^3} \left(\delta^{ns} - 3 \frac{R^n R^s}{R^2} \right) \lim_{\eta \rightarrow 0} \left\{ \int_{-\infty}^\infty dx \frac{x}{x + x_1} \frac{e^{ix - \eta|x|}}{2} + \int_{-\infty}^\infty dx \frac{x}{x + x_1} \frac{e^{-ix - \eta|x|}}{2} \right\} \\ &+ \frac{1}{R^3} \left(\delta^{ns} - 3 \frac{R^n R^s}{R^2} \right) \lim_{\eta \rightarrow 0} \left\{ \int_{-\infty}^\infty dx \frac{1}{x + x_1} \frac{e^{ix - \eta|x|}}{2i} - \int_{-\infty}^\infty dx \frac{1}{x + x_1} \frac{e^{-ix - \eta|x|}}{2i} \right\}, \end{aligned} \quad (29)$$

where we have introduced a convergence factor $e^{-\eta|x|}$ to make our integrands divergence-free.

It is quite surprising that the principal-value integrals in Eq. (29) can be evaluated using Cauchy's residue theorem (see Fig. 2). One identifies the principal-value evaluation with a symmetric encircling of the pole, on a half-circle either above or below the pole

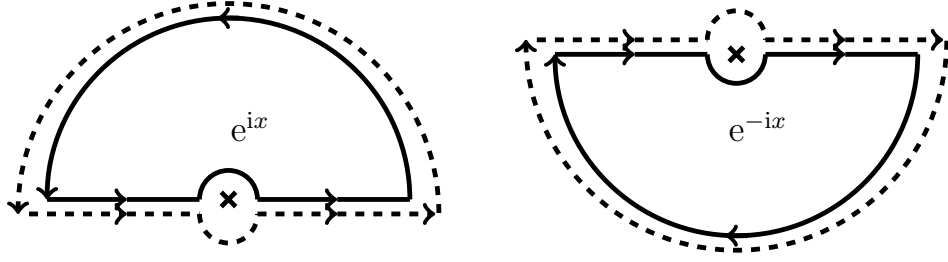


Figure 2. Complex integration contours to calculate the principal value of integrals in Eq. (29).

in the complex plane, and then closes the contour in the appropriate half of the complex plane, as dictated by the functional form of the exponential [$\exp(ix) \rightarrow$ upper half, $\exp(-ix) \rightarrow$ lower half]. We finally take the limit $\eta \rightarrow 0$ at the end, which yields

$$\int_{-\infty}^{\infty} dk_2 k_2^3 \frac{A^{ns}(k_2 R)}{(k_1 + k_2)} = \frac{1}{R^3} \left(\delta^{ns} - \frac{R^n R^s}{R^2} \right) \pi x_1^2 \cos x_1 - \frac{1}{R^3} \left(\delta^{ns} - 3 \frac{R^n R^s}{R^2} \right) \times (\pi x_1 \sin x_1 - \pi \cos x_1). \quad (30)$$

Rearranging Eq. (30) and replacing the assumed variable x_1 by its value $x_1 = k_1 R$, one obtains

$$\int_{-\infty}^{\infty} dk_2 k_2^3 \frac{A(k_2 R)}{(k_1 + k_2)} = \pi k_1^3 \left[\left(\delta^{ns} - \frac{R^n R^s}{R^2} \right) \frac{\cos k_1 R}{k_1 R} - \left(\delta^{ns} - 3 \frac{R^n R^s}{R^2} \right) \times \left(\frac{\sin k_1 R}{(k_1 R)^2} + \frac{\cos k_1 R}{(k_1 R)^3} \right) \right], \quad (31)$$

which we substitute to Eq. (28) and carry out the algebra to get

$$E_L(R) = -\frac{e^4}{72\pi^3} \sum_{\rho, \sigma} \sum_{j, \ell} \frac{\langle \phi_{1S,A} | x^j | \rho \rangle \langle \rho | x^j | \phi_{1S,A} \rangle \langle \phi_{1S,B} | x^\ell | \sigma \rangle \langle \sigma | x^\ell | \phi_{1S,B} \rangle}{(E_{A\rho} + E_{B\sigma})} \times \int_0^\infty dk_1 k_1^6 \frac{(E_{A\rho} + E_{B\sigma} + 2k_1)}{(E_{B\sigma} + k_1)(E_{A\rho} + k_1)} \left[\frac{\sin 2k_1 R}{(k_1 R)^2} - \frac{2 \sin^2 k_1 R}{(k_1 R)^3} + \frac{2 \cos^2 k_1 R}{(k_1 R)^3} - \frac{5 \sin 2k_1 R}{(k_1 R)^4} - \frac{6 \cos^2 k_1 R}{(k_1 R)^5} + \frac{6 \sin^2 k_1 R}{(k_1 R)^5} + \frac{3 \sin 2k_1 R}{(k_1 R)^6} \right]. \quad (32)$$

We now express the trigonometric sine and cosine functions in Eq. (32) as exponentials,

$$E_L(R) = \frac{-e^4}{72\pi^3} \sum_{\rho, \sigma} \sum_{j, \ell} \frac{\langle \phi_{1S,A} | x^j | \rho \rangle \langle \rho | x^j | \phi_{1S,A} \rangle \langle \phi_{1S,B} | x^\ell | \sigma \rangle \langle \sigma | x^\ell | \phi_{1S,B} \rangle}{E_{A\rho} + E_{B\sigma}} \frac{1}{2i} \left[\int_0^\infty dk_1 e^{2ik_1 R} \times \frac{k_1^6 (E_{A\rho} + E_{B\sigma} + 2k_1)}{(E_{B\sigma} + k_1)(E_{A\rho} + k_1)} \left\{ \frac{1}{(k_1 R)^2} + \frac{2i}{(k_1 R)^3} - \frac{5}{(k_1 R)^4} - \frac{6i}{(k_1 R)^5} + \frac{3}{(k_1 R)^6} \right\} - \int_0^\infty dk_1 k_1^6 \times \frac{(E_{A\rho} + E_{B\sigma} + 2k_1) e^{-2ik_1 R}}{(E_{B\sigma} + k_1)(E_{A\rho} + k_1)} \left\{ \frac{1}{(k_1 R)^2} - \frac{2i}{(k_1 R)^3} - \frac{5}{(k_1 R)^4} + \frac{6i}{(k_1 R)^5} + \frac{3}{(k_1 R)^6} \right\} \right]. \quad (33)$$

Let us introduce a new variable ω which has values $\omega = -ik_1$ in the first k_1 -integral and $\omega = ik_1$ in the second k_1 -integral inside the square bracket $[\]$ in Eq. (33). This

amounts to a Wick rotation [11], which can be carried out without problems because we are dealing with ground-state atoms,

$$\begin{aligned}
E_L(R) &= -\frac{e^4}{72\pi^3} \int_0^\infty d\omega \frac{\omega^4 e^{-2\omega R}}{R^2} \sum_{\rho,j} E_{A\rho} \frac{\langle \phi_{1S,A} | x^j | \rho \rangle \langle \rho | x^j | \phi_{1S,A} \rangle}{(E_{A\rho}^2 + \omega^2)} \\
&\quad \times \sum_{\sigma,\ell} E_{B\sigma} \frac{\langle \phi_{1S,B} | x^\ell | \sigma \rangle \langle \sigma | x^\ell | \phi_{1S,B} \rangle}{(E_{B\sigma}^2 + \omega^2)} \left[1 + \frac{2}{\omega R} + \frac{5}{(\omega R)^2} + \frac{6}{(\omega R)^3} + \frac{3}{(\omega R)^4} \right] \\
&= -\frac{1}{32\pi^3} \int_0^\infty d\omega \alpha_A(i\omega) \alpha_B(i\omega) \frac{\omega^4 e^{-2\omega R}}{R^2} \left[1 + \frac{2}{\omega R} + \frac{5}{(\omega R)^2} + \frac{6}{(\omega R)^3} + \frac{3}{(\omega R)^4} \right], \quad (34)
\end{aligned}$$

where the quantities $\alpha_A(i\omega)$ and $\alpha_B(i\omega)$ are the dynamic ground-state polarizabilities of atoms A and B , respectively,

$$\alpha_A(i\omega) = \frac{2e^2}{3} \sum_{\rho,j} \frac{E_{A\rho}}{(E_{A\rho}^2 + \omega^2)} \langle \phi_{1S,A} | x^j | \rho \rangle \langle \rho | x^j | \phi_{1S,A} \rangle, \quad (35a)$$

$$\alpha_B(i\omega) = \frac{2e^2}{3} \sum_{\sigma,\ell} \frac{E_{B\sigma}}{(E_{B\sigma}^2 + \omega^2)} \langle \phi_{1S,B} | x^\ell | \sigma \rangle \langle \sigma | x^\ell | \phi_{1S,B} \rangle. \quad (35b)$$

The dynamic polarizabilities given in Eqs. (35a) and (35b) can be rewritten as

$$\alpha_A(i\omega) = \frac{e^2}{3} \sum_{\pm,j} \langle \phi_{1S,A} | x^j \frac{1}{H - E_{1S,A} \pm i\omega} x^j | \phi_{1S,A} \rangle = \sum_{\pm} P_{1S,A}(\pm i\omega), \quad (36a)$$

$$\alpha_B(i\omega) = \frac{e^2}{3} \sum_{\pm,\ell} \langle \phi_{1S,B} | x^\ell \frac{1}{H - E_{1S,B} \pm i\omega} x^\ell | \phi_{1S,B} \rangle = \sum_{\pm} P_{1S,B}(\pm i\omega), \quad (36b)$$

with an obvious definition of the polarizability matrix elements P . For large ω , the polarizabilities show ω^{-2} behavior. The expression for the Casimir-Polder interaction energy between any two atoms A and B from the six time-ordered diagrams of the “ladder” type (I, III, IV, VII, IX, and X in Fig. 2) is thus given by

$$E_L(R) = -\frac{1}{32\pi^3} \int_0^\infty d\omega \alpha_A(i\omega) \alpha_B(i\omega) \frac{\omega^4 e^{-2\omega R}}{R^2} \left[1 + \frac{2}{\omega R} + \frac{5}{(\omega R)^2} + \frac{6}{(\omega R)^3} + \frac{3}{(\omega R)^4} \right], \quad (37)$$

Here we have used $e^2 = 4\pi\alpha$ which holds in the natural units, and we remark that Eq. (37) is valid for any interatomic separation R provided their wave functions do not overlap.

Interestingly, the $E_L(R)$ is one half of the total Casimir-Polder interaction energy between two atoms. (see Refs. [11], Chap. 85 of Ref. [15], or Ref. [16]). The other half to the Casimir-Polder interaction, denoted here as $E_C(R)$, where the subscript “C” stands for cross, comes from the remaining six-time-ordered diagrams in which photon lines cross, namely, II, V, VI, VIII, XI, and XII in Fig. 1. One can perform a separate evaluation of these crossed diagrams, along the same ideas as discussed above (in particular, the integration contours in Fig. 2 are useful). Skipping further details, it is useful to point out that the contribution of the six time-ordered diagrams with crossed photon lines is just the same as the one from the ladder diagrams, i.e., that $E_C(R) = E_L(R)$.

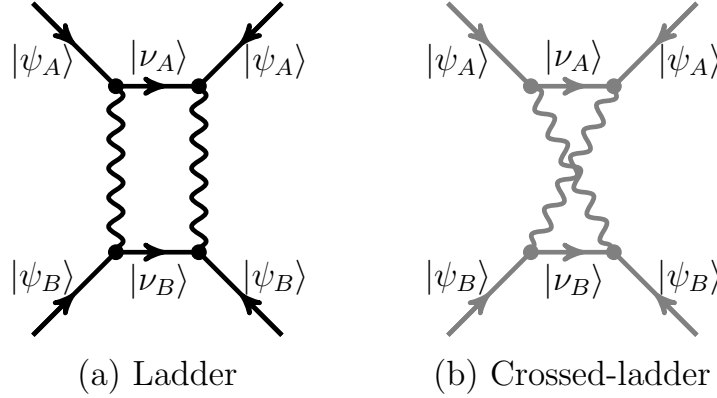


Figure 3. The ladder (a) and crossed-ladder (b) Feynman diagrams, shaded in order to show the equivalence to the time-ordered diagrams in Fig. 1. $|\nu_A\rangle$ and $|\nu_B\rangle$ are virtual-states accessible by a dipole transition from the atomic reference states $|\psi_A\rangle$ and $|\psi_B\rangle$, respectively. The latter are chosen as the $|1S\rangle$ states in the calculations reported here

3. Covariant Formalism: Matching the Scattering Amplitude

We briefly recall the formalism used in Ref. [11], in order to identify the contribution of the crossed and ladder diagrams to the Casimir–Polder interaction energy. To the fourth-order, the contribution to the scattering operator, \hat{S} , is given by the following expression (see Eq. (5) of Ref [11])

$$\hat{S}^{(4)} = \frac{1}{24} \int_{-\infty}^{\infty} dt_1 \int_{-\infty}^{\infty} dt_2 \int_{-\infty}^{\infty} dt_3 \int_{-\infty}^{\infty} dt_4 \hat{T}[V(t_1)V(t_2)V(t_3)V(t_4)], \quad (38)$$

where \hat{T} denotes the time ordering operator. In the dipole approximation, the interaction Hamiltonian $V(t) = \hat{H}_{AB}$ (see Eq. (7)) can be conveniently expressed as

$$V(t) \approx -\vec{d}_A \cdot \vec{E}(\vec{R}_A, t) - \vec{d}_B \cdot \vec{E}(\vec{R}_B, t), \quad (39)$$

where $\vec{d}_i = e\vec{r}_i$ is the electric dipole operator for atom i whose nucleus is at \vec{R}_i , and this time, we explicitly indicate the time-dependence of the interaction Hamiltonian, employing interaction-picture field operators. Assuming that the unperturbed state of the system contains atoms on the state $|\psi\rangle = |\psi_A, \psi_B\rangle$ and the electromagnetic field in the vacuum state $|0\rangle$, the fourth-order forward-scattering S -matrix element is given by

$$\langle S^{(4)} \rangle = \langle \psi | \langle 0 | \hat{S}^{(4)} | 0 \rangle | \psi \rangle. \quad (40)$$

The time ordering of the electric-field operators in Eq. (38) leads to the photon propagators, while the four types of contributions which arise due to time orderings of electric dipole moment operators in the interactions $V(t_i)$ are given in Eq. (6) of Ref. [11], which read as follows:

$$C_1 \equiv \langle \psi_A | \hat{T}_d d_{Ai}(t_1) d_{Ak}(t_3) | \psi_A \rangle \langle \psi_B | \hat{T}_d d_{Bj}(t_2) d_{B\ell}(t_4) | \psi_B \rangle, \quad (41a)$$

$$C_2 \equiv \langle \psi_A | \hat{T}_d d_{Ai}(t_1) d_{A\ell}(t_4) | \psi_A \rangle \langle \psi_B | \hat{T}_d d_{Bj}(t_2) d_{Bk}(t_3) | \psi_B \rangle, \quad (41b)$$

$$C_3 \equiv \langle \psi_B | \hat{T}_d d_{Bi}(t_1) d_{B\ell}(t_4) | \psi_B \rangle \langle \psi_A | \hat{T}_d d_{Aj}(t_2) d_{Ak}(t_3) | \psi_A \rangle, \quad (41c)$$

$$C_4 \equiv \langle \psi_B | \hat{T}_d d_{Bi}(t_1) d_{Bk}(t_3) | \psi_B \rangle \langle \psi_A | \hat{T}_d d_{Aj}(t_2) d_{A\ell}(t_4) | \psi_A \rangle, \quad (41d)$$

where \hat{T}_d is the time ordering operator for the dipole moments. The graph (a) of Fig. 3 represents the sum of the contributions C_1 and C_3 , while the other two contributions, viz. C_2 and C_4 come from the graph (b). All terms given in Eq. (3) are multiplied by two photon propagators of the index structure “12” and “34”, respectively, and, hence, give identical contributions to the S matrix element, as explained in detail in Ref. [11]. Consequently, the ladder $\langle S^{(4)} \rangle_L$ and the crossed-ladder $\langle S^{(4)} \rangle_C$ contributions to the scattering matrix element can be written as

$$\begin{aligned} \langle S^{(4)} \rangle_L = \langle S^{(4)} \rangle_C &= \frac{1}{4} \int_{-\infty}^{\infty} dt_1 \int_{-\infty}^{\infty} dt_2 \int_{-\infty}^{\infty} dt_3 \int_{-\infty}^{\infty} dt_4 \langle 0 | \hat{T}_E \left[E_i(\vec{R}_A, t_1) E_j(\vec{R}_B, t_2) \right] | 0 \rangle \\ &\times \langle 0 | \hat{T}_E \left[E_k(\vec{R}_A, t_3) E_\ell(\vec{R}_B, t_4) \right] | 0 \rangle \langle \psi_A | \hat{T}_d \left[d_{Ai}(t_1) d_{Ak}(t_3) \right] | \psi_A \rangle \\ &\times \langle \psi_B | \hat{T}_d \left[d_{Bj}(t_2) d_{B\ell}(t_4) \right] | \psi_B \rangle. \end{aligned} \quad (42)$$

At this point, we could stop the calculation and argue that, since the S matrix elements generated by the crossed and ladder diagrams are the same, the effective Hamiltonians and energy shifts corresponding to the diagrams also must be the same, proving consistency with the results of Sec. 2. However, we carry through the derivation for completeness. We recall that \hat{T}_E is the time ordering operator for the electric field operators. According to Eqs. (18) and (21) of Ref. [11], one may carry out the t -integrals of Eq. (42), which finally gives

$$\langle S^{(4)} \rangle_L = \frac{T}{4} \int_{-\infty}^{\infty} \frac{d\omega}{2\pi} \omega^4 D_{ij}(\omega, \vec{R}) D_{k\ell}(\omega, \vec{R}) \alpha_{A,ik}(\omega) \alpha_{B,j\ell}(\omega), \quad (43)$$

where $T = \int_{t_i}^{t_f} dt = t_f - t_i$ denotes the total interval of time in which the transition occurs. The photon propagator, or, merely, as explained in Ref. [11], electric-field propagator, $D_{ij}(\omega, \vec{R})$, can be expressed in terms of the tensor structures α_{ij} and β_{ij} ,

$$D_{ij}(\omega, \vec{R}) = \frac{e^{i|\omega|R}}{4\pi} \left[\alpha_{ij} - \beta_{ij} \left(\frac{i}{|\omega|R} - \frac{1}{\omega^2 R^2} \right) \right], \quad (44)$$

where

$$\alpha_{ij} = \delta_{ij} - \frac{R_i R_j}{R^2}, \quad \text{and} \quad \beta_{ij} = \delta_{ij} - 3 \frac{R_i R_j}{R^2}. \quad (45)$$

The dynamic polarizability $\alpha_{A,ik}(\omega)$ in Eq. (43) is given as

$$\alpha_{A,ik}(\omega) = \sum_{\nu_A} \left(\frac{\langle \psi_A | d_{Ai} | \nu_A \rangle \langle \nu_A | d_{Aj} | \psi_A \rangle}{E_{\nu_A} - \omega - i\epsilon} + \frac{\langle \psi_A | d_{Ai} | \nu_A \rangle \langle \nu_A | d_{Aj} | \psi_A \rangle}{E_{\nu_A} + \omega - i\epsilon} \right). \quad (46)$$

The matching relation for the diagonal element of the effective Hamiltonian H_{eff} (“quasipotential”) derived from an S matrix element is (see Eq. (3) of Ref. [11])

$$\langle S^{(4)} \rangle = -iT \langle \psi | H_{\text{eff}} | \psi \rangle, \quad (47)$$

so that, for the contribution of the ladder Feynman diagram of $\langle \psi | H_{\text{eff}} | \psi \rangle = E_L(R)$, one has in view of Eq. (43)

$$E_L(R) = \frac{i}{2} \int_0^\infty \frac{d\omega}{2\pi} \omega^4 D_{ij}(\omega, \vec{R}) D_{k\ell}(\omega, \vec{R}) \alpha_{A,ik}(\omega) \alpha_{B,j\ell}(\omega). \quad (48)$$

For a reference $1S$ state, one has $\alpha_{A,ik}(\omega) = (\delta^{ik}/3) \alpha_A(\omega)$. Under a Wick-rotation $\omega \rightarrow i\omega$, Eq. (48) reads as

$$E_L(R) = -\frac{1}{32\pi^3} \int_0^\infty d\omega \alpha_A(i\omega) \alpha_B(i\omega) \frac{\omega^4 e^{-2\omega R}}{R^2} \times \left[1 + \frac{2}{\omega R} + \frac{5}{(\omega R)^2} + \frac{6}{(\omega R)^3} + \frac{3}{(\omega R)^4} \right]. \quad (49)$$

Note that, $E_L(R)$ is half of the total interaction energy, confirming the consistency with the result reported in Sec. 2, which implies that the ladder-type diagrams contribute exactly half of the Casimir-Polder interaction.

4. Radiative Corrections

Relativistic corrections to the leading-order expression

$$E(R) = E_L(R) + E_C(R) = -\frac{1}{16\pi^3} \int_0^\infty d\omega \alpha_A(i\omega) \alpha_B(i\omega) \frac{\omega^4 e^{-2\omega R}}{R^2} \times \left[1 + \frac{2}{\omega R} + \frac{5}{(\omega R)^2} + \frac{6}{(\omega R)^3} + \frac{3}{(\omega R)^4} \right]. \quad (50)$$

involve corrections to the atomic Hamiltonian, to the energy, to the wave function, and to the transition current [6]. In units with $\hbar = c = \epsilon_0 = 1$, which are used throughout this article, the Bohr radius is $a_0 = (\alpha m)^{-1}$, and the interatomic distance, expressed in atomic units, is

$$\rho = \frac{R}{a_0} = \alpha m R. \quad (51)$$

One can write (see Ref. [6]) a systematic expansion of the interaction energy, which clarifies the relevant orders of the expansion in powers of the fine-structure constant α . In the non-retardation regime, one encounters the following terms [see Eq. (29) of Ref. [6]]

$$E(\alpha, mR) = E_{\text{free}}(\alpha) - \sum_{i,j} m\alpha^i \frac{C_j^{(i)}}{(m\alpha R)^j} = E_{\text{free}}(\alpha) - \sum_{i,j} m\alpha^i \frac{C_j^{(i)}}{\rho^j}, \quad (52)$$

where $E_{\text{free}}(\alpha)$ refers to the α -expansion of the sum of the free (non-interacting) energies of the two atoms. [For a conjectured necessary generalization of this expansion, see Eq. (80) below.]

The leading term from the Casimir-Polder interaction is proportional to $C_6^{(2)}$, and equal to the van der Waals energy. Here, we recall that in our units, the Hartree energy is expressed as $E_h = \alpha^2 m$. In the non-retardation regime, the quadrupole term gives a correction proportional to $C_8^{(2)}$ (see Eq. (33) of Ref. [6]). Surprisingly, this term is not suppressed by a factor of α , but by a higher power of the scaled interatomic distance ρ (eighth power instead of sixth). The relativistic corrections to the Hamiltonian, energy and wave function, together with the dipole-octupole mixing term and the relativistic corrections to the current, give the term $C_6^{(4)}$, which is still proportional to $1/\rho^6$, but has a prefactor $m\alpha^4$ instead of $m\alpha^2$, and is thus suppressed by

two powers of α . We find that the radiative correction to the Casimir-Polder interaction contributes, in the non-retardation regime, to the coefficient $C_6^{(5,1)}$, with a prefactor proportional to $\alpha^5 m \ln(\alpha^{-2})$. (The single power of the logarithm is denoted here by the second upper index of the coefficient, inspired by a commonly accepted notation adopted in Lamb shift calculations [17].)

In order to obtain the leading radiative correction, we use the “effective radiative Lamb shift potential” (see Ref. [19]), denoted as δV_{Lamb} ,

$$\delta V_{\text{rad}} = \frac{4\alpha}{3\pi} [\pi\alpha] \ln[\alpha^{-2}] \frac{\delta^{(3)}(\vec{r})}{m^2} = \frac{4\alpha}{3\pi} \ln[\alpha^{-2}] \delta V, \quad (53)$$

where δV is a “standard potential” whose expectation value, on a hydrogenic state, has particularly simple prefactors,

$$\delta V = \frac{\pi\alpha}{m^2} \delta^{(3)}(\vec{r}) = \pi\alpha^4 m \delta^{(3)}\left(\frac{\vec{r}}{a_0}\right), \quad \langle nS | \delta V | nS \rangle = \frac{(\alpha m)^3}{n^3}. \quad (54)$$

We recall that only S states are nonvanishing at the origin. We then perturb the Hamiltonian, energy, and reference state, by the radiative Lamb shift potential, in both atoms A and B . We will study the corresponding radiative shift for two hydrogen atoms, which are both in their ground state. The modification of the total Casimir-Polder interaction can be written as

$$\begin{aligned} \delta E(R) = & -\frac{2}{\pi(4\pi)^2} \int_0^\infty d\omega \alpha_A(i\omega) \delta\alpha_B(i\omega) \frac{\omega^4 e^{-2\omega R}}{R^2} \\ & \times \left[1 + \frac{2}{\omega R} + \frac{5}{(\omega R)^2} + \frac{6}{(\omega R)^3} + \frac{3}{(\omega R)^4} \right], \end{aligned} \quad (55)$$

where $\delta\alpha_B$ is the perturbation of the polarizability due to the “standard potential” (54),

$$\delta\alpha_B(i\omega) = \sum_{\pm} \delta P_{1S}(\pm i\omega). \quad (56)$$

Here, δP_{1S} is the δV -induced perturbation of the polarizability matrix element defined in Eq. (2), for atom B . The perturbed P -matrix δP_{1S} element has three contributions, namely, corrections to the Hamiltonian of the propagator denominator, the energy, and the wave function. Explicitly,

$$\delta P_{1S}(i\omega) = \delta P_{1S}^{(H)}(i\omega) + \delta P_{1S}^{(E)}(i\omega) + \delta P_{1S}^{(\phi)}(i\omega), \quad (57)$$

The correction arising from the Hamiltonian reads

$$\delta P_{1S}^{(H)}(i\omega) = -\frac{e^2}{3} \left\langle 1S \left| x^i \frac{1}{H - E_{1S} + i\omega} \delta V \frac{1}{H - E_{1S} - i\omega} x^i \right| 1S \right\rangle, \quad (58)$$

which is zero as the matrix element of the Dirac- δ between any two virtual P states vanishes. The contribution to the Casimir-Polder interaction from the correction to the energy is given by

$$\delta P_{1S}^{(E)}(i\omega) = -\frac{\partial}{\partial \omega} P_{1S}(i\omega) \langle 1S | \delta V | 1S \rangle = -\alpha^4 m \frac{\partial}{\partial \omega} P_{1S}(i\omega), \quad (59)$$

The modification of the P -matrix element due to the wave function correction, to the first order, is given by

$$\delta P_{1S}^{(\phi)}(i\omega) = \frac{2}{3} e^2 \left\langle 1S \left| x^i \frac{1}{H - E_{1S} + i\omega} x^i \right| \delta(1S) \right\rangle, \quad (60)$$

where the perturbed $1S$ -state wave function is

$$|\delta(1S)\rangle = \frac{1}{(E_{1S} - H)'} \delta V |1S\rangle. \quad (61)$$

In coordinate space, one has

$$\delta\Psi_{1S}(\vec{r}) = \frac{1}{\sqrt{4\pi}} \delta R_{10}(r) = 2\alpha^2 \frac{e^{-r/a_0}}{3\pi\sqrt{\pi a_0}} \left[-\frac{1}{r} - \frac{1}{a_0} \left(5 - 2\gamma_E - 2 \ln \left(\frac{r}{a_0} \right) \right) + \frac{2r}{a_0^2} \right], \quad (62)$$

where $\gamma_E = 0.577\,2157$ is the Euler–Mascheroni constant. The result (62) is in agreement with Eq. (23) of Ref. [20].

4.1. Short Range

In the short-range regime, i.e., $1/(\alpha m) \ll R \ll 1/(\alpha^2 m)$, the radiative correction to the interaction energy takes the form

$$\begin{aligned} \delta E_{\text{rad}}(\alpha, mR) &= -\frac{6}{\pi(4\pi)^2 R^6} \int_0^\infty d\omega \alpha_{1S}(i\omega) \delta\alpha_{1S}(i\omega) \frac{4\alpha}{3\pi} \ln(\alpha^{-2}) \\ &= -\frac{4}{3\pi} \alpha^3 m \ln(\alpha^{-2}) \frac{\delta X^{\text{dl}}}{(\alpha m R)^6}, \end{aligned} \quad (63)$$

where the delta-perturbed van der Waals δX^{dl} coefficient (“dl” stands for dimensionless, i.e., expressed in atomic units) is given by

$$\begin{aligned} \delta X^{\text{dl}} &= \frac{6}{\pi} \int_0^\infty d\omega \alpha_{1S}^{\text{dl}}(i\omega) \delta\alpha_{1S}^{\text{dl}}(i\omega) \\ &= \frac{6}{\pi} \int_0^\infty d\omega \alpha_{1S}^{\text{dl}}(i\omega) \left(\delta\alpha_{1S}^{(E,\text{dl})}(i\omega) + \delta\alpha_{1S}^{(\phi,\text{dl})}(i\omega) \right). \end{aligned} \quad (64)$$

Here E , ϕ , and dl stand for the energy correction, the wave function part, and the dimensionless quantity respectively. One can use convergence acceleration techniques as discussed in Refs. [21,22] in addition to other numerical methods presented in Ref. [17] and evaluate the integral (64) numerically, which yields

$$\delta X^{\text{dl}} = 69.371\,0888 \alpha^2. \quad (65)$$

The radiative correction to the interaction energy can be expressed as

$$\delta E_{\text{rad}}(\alpha, mR) = -\alpha^5 m \frac{\delta C_6^{(5)}}{(\alpha m R)^6}, \quad (66)$$

where

$$\delta C_6^{(5)} = 29.442\,0042 \ln(\alpha^{-2}) \quad (67)$$

is a large coefficient, which, in addition, also contains a logarithm of the fine-structure constant. The large magnitude of the logarithmic coefficient multiplying the radiative correction, which amounts to an approximate numerical value of $30 \times \ln(137^2) \approx 300$, compensates the additional power of α in comparison to the relativistic corrections considered in Ref. [6]; this implies that the effect is of the same order-of-magnitude as the relativistic corrections considered in Ref. [6] and should be included in any precise

theory of the interatomic interaction. In a wider context, the emergence of logarithmic terms in an accurate treatment of the interatomic interaction, in both the interatomic distance as well as the fine-structure constant, is discussed in the Appendix. On the other hand, in the short-range regime, the interaction energy $E(\alpha, mR)$ is given by [18]

$$E(\alpha, mR) = -\frac{3\alpha^2}{\pi e^4 R^6} \int_0^\infty d\omega \alpha_{1S}(i\omega) \alpha_{1S}(i\omega) = -\alpha^2 m \frac{C_6^{(2)}}{(\alpha m R)^6}. \quad (68)$$

where $C_6^{(2)} = 6.499\,0267$. (In obtaining numerical results, we treat the hydrogen atoms in the non-recoil limit, i.e., in the limit of an infinite mass of the nucleus.) Comparing $\delta E_{\text{rad}}(\alpha, mR)$ of Eq. (66) to $E(\alpha, mR)$ as given in Eq. (68), one can conclude that the correction to the Casimir-Polder interaction due to the leading radiative correction is of relative order $\alpha^3 \ln(\alpha^{-2})$.

4.2. Long Range

In the long-range limit, i.e., $R \gg 1/(\alpha^2 m)$, however, the dynamic polarizability of the ground state can be approximated by its static polarizability. Consequently, the Casimir-Polder interaction and the radiative correction to the Casimir-Polder interaction read

$$E(\alpha, mR) = -\alpha_A(0) \alpha_B(0) f(R), \quad (69)$$

$$\delta E_{\text{rad}}(\alpha, mR) = -2\alpha_A(0) \delta\alpha_B(0) \frac{4\alpha}{3\pi} \ln(\alpha^{-2}) f(R), \quad (70)$$

where the function $f(R)$ is an integral over the angular frequency ω ,

$$f(R) = \frac{1}{16\pi^3 R^2} \int_0^\infty d\omega \omega^4 e^{-2\omega R} \left[1 + \frac{2}{\omega R} + \frac{5}{(\omega R)^2} + \frac{6}{(\omega R)^3} + \frac{3}{(\omega R)^4} \right] = \frac{23}{(4\pi)^3 R^7}. \quad (71)$$

The ground state static polarizability $\alpha_A(0)$ of atom A , in the case of hydrogen, is given by

$$\alpha_A(0) = \frac{9e^2}{2\alpha^4 m^3}. \quad (72)$$

The δV -perturbed ground state static polarizability $\delta\alpha_B(0) = \delta\alpha_{1S}(0)$ is the sum

$$\delta\alpha_{1S}(0) = \delta\alpha_{1S}^{(E)}(0) + \delta\alpha_{1S}^{(\phi)}(0) = \frac{167e^2}{46\alpha^2 m^3}, \quad (73)$$

where

$$\delta\alpha_{1S}^{(E)}(0) = \frac{43e^2}{23\alpha^2 m^3}, \quad \delta\alpha_{1S}^{(\phi)}(0) = \frac{81e^2}{46\alpha^2 m^3}, \quad (74)$$

are, respectively, the energy and the wave function parts of delta perturbed ground state static polarizability. As a result, we have, in natural units,

$$E(\alpha, mR) = -\alpha^8 m \frac{1863}{16\pi} \frac{1}{(m\alpha^2 R)^7}, \quad (75)$$

$$\delta E_{\text{rad}}(\alpha, mR) = -\alpha^8 m \frac{501}{2\pi^2} \frac{\alpha^3 \ln(\alpha^{-2})}{(m\alpha^2 R)^7}. \quad (76)$$

It is evident from Eqs. (75) and (76) that, in the long-range, the Casimir-Polder interaction and the perturbed Casimir-Polder interaction vary as inverse seventh powers

of the interatomic distance, and the leading-order radiative correction to the Casimir-Polder interaction is of relative order $\alpha^3 \ln(\alpha^{-2})$.

5. Conclusions

We have analyzed the Casimir-Polder interaction between two neutral hydrogen atoms in the ground state. This process entails the exchange of two virtual photons. The topologically distinct 12 time-ordered diagrams are grouped into two equal halves on the basis of the presence of crossing in the photon-lines (see Sec. 2). The contribution E_L of the six “ladder” diagrams, in which the photon lines do not cross, is seen to be equal to the contribution E_C of the six diagrams with crossing photon lines.

Within the framework of covariant form of Quantum Electrodynamics, all of these twelve time-ordered diagrams can be replaced by just two Feynman diagrams (Sec. 3). The contribution of the ladder Feynman diagram is seen to equal the contribution of the six “ladder” diagrams (without crossed photon lines) in the time-ordered formalism. In addition to this, the time-ordering formalism and the covariant formalism yield identical results for the total Casimir-Polder interaction.

In Sec. 4, we discuss a systematic expansion of the Casimir-Polder interaction energy in powers of the interatomic distance, and of the fine-structure constant. In the sense of Eq. (52), we find that the radiative correction to the Casimir-Polder interaction contributes, in the non-retardation regime, to the coefficient $C_6^{(5,1)}$, with a logarithmic factor. Specifically, it is proportional to $\alpha^5 m \ln(\alpha^{-2})/\rho^6$, where ρ is the interatomic distance, measured in atomic units (see Eq. (51)). (The one power of the logarithm is denoted here by the second upper index of the coefficient.) As a consequence, the radiative correction is of relative order $\alpha^3 \ln(\alpha^{-2})$.

Our detailed calculation in the time-ordered formalism, as outlined in Sec. 2, crucially depends on the correctness of the principal-value prescription used in the evaluation of the k_1 and k_2 integrals given in Eq. (29). This treatment is restricted in validity to the ground-state interaction, where no additional poles due to virtual resonant transitions to energetically lower virtual states are available [11]. As much as our calculation shows the mutual consistency of the time-ordered, and the Feynman diagram treatment (the latter profits from the matching of the scattering amplitude), it also highlights the limitations of the time-ordered formalism, which avoids making concrete statements regarding the correct placement of the poles of the atomic Green function.

Acknowledgments

This research has been Supported by the National Science Foundation (grant PHY-1710856).

A. Appendix

We recall, for convenience, the most general form of the interatomic Casimir-Polder interaction in term of the dynamic polarizabilities from Eq. (50), where we introduce the variable $x = 2\omega R$,

$$E(R) = - \int_0^\infty \frac{dx e^{-x} (48 + 48x + 20x^2 + 4x^3 + x^4)}{512\pi^3 R^7} \alpha_A \left(\frac{ix}{2R} \right) \alpha_B \left(\frac{ix}{2R} \right). \quad (77)$$

We would like to find an expansion of this expression in the range $R > a_0 = 1/(\alpha m)$, but not necessarily $R \gg a_0$. One may use the expression in terms of oscillator strengths f_{nA} for the dynamic polarizability $\alpha_A(i\omega)$,

$$\alpha_A(i\omega) = \sum_n \frac{f_{nA}}{\omega_{nA}^2 + \omega^2}, \quad (78)$$

and analogously for atom B . For a hydrogen atom in the ground states, the oscillator strength f_{nA} is given as

$$f_{nA} = \frac{2e^2}{3} E_{nA} |\langle 0 | \vec{r}_A | n \rangle|^2, \quad (79)$$

and otherwise one has to sum over the coordinates of the atomic electrons.

In the interatomic distance range relevant to the van der Waals interaction, we seek to find the coefficients in the expansion [see Eq. (52) here and Eq. (29) of Ref. [6]]

$$E(\alpha, mR) = - \sum_{i,j} m\alpha^i \frac{C_j^{(i)}}{(\alpha mR)^j}, \quad (80)$$

where we ignore the free atomic energy. We here conjecture that the functional form given in Eq. (80) should be augmented by logarithmic terms,

$$E(\alpha, mR) = - \sum_{i,j,k} m\alpha^i \frac{C_j^{(i,k)} \ln^k(\alpha mR)}{(\alpha mR)^j}. \quad (81)$$

The $C_j^{(i)}$ coefficients are a special case of the $C_j^{(i,k)}$ for $k = 0$. In order to bring the expressions for the coefficients into a convenient form, one scales variables according to

$$\vec{r}_A = a_0 \vec{\rho}_A, \quad \vec{r}_B = a_0 \vec{\rho}_B, \quad \vec{p}_A = \frac{1}{a_0} \vec{P}_A, \quad \vec{p}_B = \frac{1}{a_0} \vec{P}_B, \quad (82)$$

$$H_A = E_h \mathcal{H}_A, \quad H_B = E_h \mathcal{H}_B, \quad E_A = E_h \mathcal{E}_A, \quad E_B = E_h \mathcal{E}_B, \quad (83)$$

where $a_0 = 1/(\alpha m)$ is the Bohr radius, and $E_h = \alpha^2 m$ is the Hartree energy. Furthermore,

$$\rho = \alpha m R = R/a_0 \quad (84)$$

is the interatomic distance, expressed in Bohr radii. The advantage of the scaled variables $\vec{\rho}_{A,B}$, $\vec{P}_{A,B}$, $\mathcal{H}_{A,B}$, and $\mathcal{E}_{A,B}$ is that they assume numerical values and expectation values of order unity, for atomic reference states and transition matrix elements. Alternatively, one might say that the scaled variables are expressed in “atomic units”.

We confirm the results given in Eqs. (30)–(32) of Ref. [6],

$$C_6^{(2,0)} = \frac{2}{3} \left\langle \rho_A^i \rho_B^j \frac{1}{\mathcal{H}_A + \mathcal{H}_B - \mathcal{E}_A - \mathcal{E}_B} \rho_A^i \rho_B^j \right\rangle, \quad (85)$$

$$C_4^{(4,0)} = \frac{2}{9} \left\langle \rho_A^i \rho_B^j \frac{1}{\mathcal{H}_A + \mathcal{H}_B - \mathcal{E}_A - \mathcal{E}_B} P_A^i P_B^j \right\rangle, \quad (86)$$

$$C_3^{(5,0)} = \frac{7}{6\pi} N_A N_B. \quad (87)$$

Here, N_A and N_B are the number of electrons in atoms A and B . Furthermore, we find the following representation for the higher-order coefficient $C_2^{(6,0)}$ emerging from Eq. (77),

$$\begin{aligned} C_2^{(6,0)} = & -\frac{1}{3} \left(N_A \langle \vec{P}_B^2 \rangle + N_B \langle \vec{P}_A^2 \rangle \right) \\ & + \frac{2}{9} \left\langle P_A^i P_B^j \frac{1}{\mathcal{H}_A + \mathcal{H}_B - \mathcal{E}_A - \mathcal{E}_B} P_A^i P_B^j \right\rangle. \end{aligned} \quad (88)$$

In the seventh order in α , a logarithmic term is obtained, which is proportional to ρ^{-1} . The mechanism behind the generation of the logarithm is that one cannot expand the integrand in Eq. (77) to arbitrarily high orders in $\omega_{nA} R$ and $\omega_{nB} R$, without incurring infrared divergences for small x . One thus has to introduce a scale-separation parameter ϵ , as in Lamb shift calculations [17, 23], to separate the region $x \ll \{\omega_{nA} R, \omega_{nB} R\}$ from the region $x \gg \{\omega_{nA} R, \omega_{nB} R\}$. Finally, one obtains the logarithmic coefficient

$$C_1^{(7,1)} = -\frac{88}{45} \left(N_A \langle \delta^{(3)}(\vec{\rho}_B) \rangle + N_B \langle \delta^{(3)}(\vec{\rho}_A) \rangle \right). \quad (89)$$

The expression for the accompanying nonlogarithmic term is more complicated and of the Bethe logarithm type,

$$\begin{aligned} C_1^{(7,0)} = & \frac{8}{675} (193 - 165 \gamma_E) \left(N_A \langle \delta^{(3)}(\vec{\rho}_B) \rangle + N_B \langle \delta^{(3)}(\vec{\rho}_A) \rangle \right) + \frac{88}{135\pi} \\ & \times \left\langle \rho_A^i \rho_B^j \frac{(\mathcal{H}_A - \mathcal{E}_A)^4 \ln(2\alpha|\mathcal{H}_A - \mathcal{E}_A|) - (\mathcal{H}_B - \mathcal{E}_B)^4 \ln(2\alpha|\mathcal{H}_B - \mathcal{E}_B|)}{(\mathcal{H}_A - \mathcal{E}_A)^2 - (\mathcal{H}_B - \mathcal{E}_B)^2} P_A^i P_B^j \right\rangle. \end{aligned} \quad (90)$$

For two identical atoms, the denominator $(\mathcal{H}_A - \mathcal{E}_A)^2 - (\mathcal{H}_B - \mathcal{E}_B)^2$ vanishes if, in a sum-over-states representation, the same excited intermediate state enters the calculation. However, the numerator in this case also becomes singular. Numerically, one could treat the problem by adding an infinitesimal shift to the Hamiltonian of atom B , as in the replacement $\mathcal{H}_B - \mathcal{E}_B \rightarrow \mathcal{H}_B - \mathcal{E}_B + \eta$, and considering the limit $\eta \rightarrow 0$ at the end of the calculation. Alternatively, for two identical atoms with $\mathcal{E}_A = \mathcal{E}_B = \mathcal{E}_0$, and $|\langle 0|\vec{\rho}_A|n_A\rangle|^2 = |\langle 0|\vec{\rho}_B|n_B\rangle|^2 = |\langle 0|\vec{\rho}|n\rangle|^2$ (for $n_A = n_B$), the contribution of the same-excitation states in both atoms yields a contribution

$$\begin{aligned} \overline{C}_1^{(7,0)} = & -\frac{44}{135\pi} \sum_n \left\{ |\langle 0|\vec{\rho}|n\rangle|^2 \right\}^2 (\mathcal{E}_n - \mathcal{E}_0)^4 [1 + 4 \ln(2\alpha|\mathcal{E}_n - \mathcal{E}_0|)] \\ = & -\frac{44}{135\pi} \sum_n \left\{ \left| \langle 0|\vec{P}|n\rangle \right|^2 \right\}^2 [1 + 4 \ln(2\alpha|\mathcal{E}_n - \mathcal{E}_0|)]. \end{aligned} \quad (91)$$

The full $C_1^{(7,0)}$ can, in this case, be obtained by adding the term $\overline{C}_1^{(7,0)}$ to the term from Eq. (90), when the sum over virtual states in the latter is restricted to virtual states with a manifestly different energy for the two atoms.

The above consideration illustrate that in higher orders, logarithmic terms (both in α as well as in R) naturally occur in calculations of the Casimir–Polder (van der Waals) interaction and need to be taken into account in a precise analysis of the problem. Furthermore, we uncover a Bethe-logarithm-like structure in the accompanying nonlogarithmic terms.

References

- [1] Casimir H B G and Polder D 1948 *Phys. Rev.* **73** 360
- [2] Jentschura U D, Adhikari C M and Debierre V 2017 *Phys. Rev. Lett.* **118** 123001
- [3] Jamieson M J, Drake G W F, and Dalgarno A 1995 *Phys. Rev. A* **51** 3358
- [4] Chen M K and Chung K T 1996 *Phys. Rev. A* **53** 1439
- [5] Yan Z C, Dalgarno A, and Babb J F 1997 *Phys. Rev. A* **55** 2882
- [6] Pachucki K 2005 *Phys. Rev. A* **72** 062706
- [7] Power E A 2001 *Eur. J. Phys.* **22** 453
- [8] Power E A and Thirunamachandran T 1995 *Phys. Rev. A* **51** 3660
- [9] Donaire M, Guerout R, and Lambrecht A 2015 *Phys. Rev. Lett.* **115** 033201
- [10] Jentschura U D, Debierre V, Adhikari C M, Matveev A, and Kolachevsky N 2017 *Phys. Rev. A* **95** 022704
- [11] Jentschura U D, Debierre V 2017 *Phys. Rev. A* **95** 042506
- [12] Jentschura U D and Keitel C H 2004 *Ann. Phys. (N.Y.)* **310** 1
- [13] Craig D P and Thirunamachandran T 1984 *Molecular quantum electrodynamics: An introduction to radiation-molecule interactions* (Academic Press, New York, NY)
- [14] Salam A 2009 *Molecular quantum electrodynamics* (John Wiley & Sons, Inc. Hoboken, NJ, 2009) 121
- [15] Berestetskii V B, Lifshitz E M and Pitaevskii L P 1982 *Quantum Electrodynamics, Volume 4 of the Course on Theoretical Physics*, 2nd Ed (Pergamon Press, Oxford, UK)
- [16] Adhikari C M 2017 *Long-range interatomic interactions: Oscillatory tails and hyperfine perturbations*, PhD thesis, Missouri University of Science and Technology, available at http://scholarsmine.mst.edu/doctoral_dissertations/2615
- [17] Jentschura U and Pachucki K 1996 *Phys. Rev. A* **54** 1853
- [18] Adhikari C M, Debierre V, Matveev A, Kolachevsky N and Jentschura U D 2017 *Phys. Rev. A* **95** 022703
- [19] Jentschura U D 2003 *J. Phys. A* **36** L229
- [20] Cohen M, Dalgarno A 1961 *Proc. Roy. Soc. London A* **261** 565.
- [21] Jentschura U D, Mohr P J, Soff G and Weniger E J 1999 *Comput. Phys. Commun.* **116** 28
- [22] Jentschura U D 2002 *Quantum electrodynamic bound-state calculations and large-order perturbation theory*, Habilitation thesis, Dresden University of Technology, available at <https://arxiv.org/pdf/hep-ph/0306153>
- [23] Pachucki K 1993 *Ann. Phys. (N.Y.)* **226** 1